ACS OMEGA

http://pubs.acs.org/journal/acsodf

Article

Synergistic and Antagonistic Effects of the Co-Pyrolysis of Plastics and Corn Stover to Produce Char and Activated Carbon

Mark Gale, Peter M. Nguyen, and Kandis Leslie Gilliard-AbdulAziz*

Cite This: *ACS Omega* 2023, 8, 380−390

Read Online

ACCESS | Metrics & More | Article Recommendations | Supporting Information

ABSTRACT: The physicochemical properties of char and activated carbon produced from the co-pyrolysis of corn stover (CS) and plastics, polystyrene (PS) and polyethylene terephthalate (PET), were studied. Non-isothermal gas analysis of the volatiles was conducted using an online mass spectrometer to correlate the thermal degradation of gaseous byproducts to the formation of pores in the char materials. The findings determined that the addition of PS or PET promotes the formation of the solid char product with either higher than average pore sizes or surface areas compared to control samples. The addition of PET to corn stover increases the surface area of the char formed. The char formed from a CS:PET mass ratio of 1:1 produced char with a surface area of 423.8 ± 24.8 m^2/g at 500 °C and a duration of 2 h. The surface area of the chars formed from CS and PET decreased as the amount of PET decreased, showing a tendency for PET to increase the surface area of the char materials synergistically. The addition of PS to corn stover promoted the formation of chars with, on average, larger pore sizes than the control char samples. The chars were chemically activated with potassium hydroxide, and the activated carbon that formed had lower surface areas but comparable surface functional groups to the control samples. Vanillin adsorption testing showed that activated carbon from corn stover performed the best at removing 95% of the vanillin after 2 h. In contrast, the activated carbon from the chars produced from the co-pyrolysis of corn stover and polystyrene or corn stover and polyethylene terephthalate removed 45% and 46% of vanillin after 2 h, respectively. The findings suggest that plastics have a synergistic relationship in producing char precursors with improved porosity but antagonistically affect the activated carbon adsorbent properties.

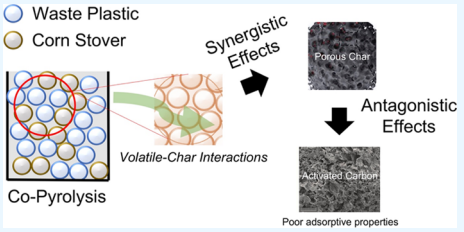

1. INTRODUCTION

The use of plastics, such as polystyrene (PS) and polyethylene terephthalate (PET), has transformed our society by providing protection and storage for food, fibers in our clothing, and containers for goods.[1] Due to PET and PS's low degradability, most plastic waste is discarded and accumulates in landfills.[2] Few PET and PS recycling strategies allow for the full utilization of monomers or reuse into relevant products. PET consists of repeating ethylene glycol and terephthalic acid monomers and is resistant to microbial degradation, posing issues with environmental remediation and extensive accumulation in the environment.[3,4] PS contains styrene monomer units that are difficult to depolymerize and can persist for over 100 years in the environment.[5,6] The stable attributes of PET and PS, with improved chemical resistance and durability, make them widely useful but exceedingly difficult to recycle. Finding ways to recycle or upcycle these plastics will be necessary to mitigate solid waste management issues.

Plastic upcycling is an emerging alternative to mechanical recycling, where plastic waste is converted to value-added chemicals or materials such as activated carbon (AC), fuels, waxes, and lubricants.[7−9] One technique to transform plastic waste into value-added products is using a thermochemical approach, pyrolysis, to break down the polymeric structure into three fractions: solid (char), liquid (pyrolysis oil), and gas, which can be valorized into chemical commodities and AC. A strategy incorporating the existing biorefinery framework seeks to include natural (cellulose, hemicellulose, and lignin) and synthetic (plastics) polymers in a process called co-pyrolysis. Co-pyrolysis involves thermoconversion of the biomass and plastic waste feeds in an oxygen-free environment with temperatures between 300 - 700 °C. Pyrolysis oil is one of the most valuable fractions used as a feed for fuels and chemical commodities.[10−12] The solid product, char, can be used as a solid fuel or modified for improved adsorptive properties as AC.[13]

During co-pyrolysis, the high hydrogen/carbon (H/C) ratios and low oxygen/carbon (O/C) of plastic wastes work synergistically with the high oxygen/carbon (O/C) and low hydrogen/carbon (H/C) of lignocellulosic biomass, improving the quality of the products formed. Certain plastics, such as PS, act as hydrogen donors in co-pyrolysis which promotes the hydrogenolysis or deoxygenation of the biomass fraction.[14−16] The synergistic relationship between plastic and biomass has

Received: July 29, 2022
Accepted: December 12, 2022
Published: December 21, 2022

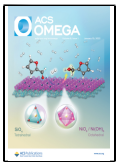

improved the oil yield, quality, and composition.[17,18] The presence of plastic not only enhances the pyrolysis oil's content but can also contribute to changes in the chemical composition, surface, and porosity of the char formed. While there have been co-pyrolysis studies on the improvement of the pyrolytic oil, few studies[16] have examined the char formed from the process to determine whether the properties are amenable for applications beyond use as a solid fuel. The quality of the char formed is primarily ignored, and additional research is needed on the formed char to optimize its properties as an adsorbent.

This study evaluates the physicochemical properties of char produced from the co-pyrolysis of corn stover with PS or PET. It assesses whether there are synergistic or antagonistic qualities that influence their use as precursors for AC. Activated carbon is used in industries such as water treatment,[19,20] air purification,[21,22] and catalysis[26,27,] often as a catalyst support[23,24] or pollution remediation. Corn stover was chosen as the lignocellulosic biomass candidate as it is among the top agricultural waste byproducts produced in the United States. PS and PET were selected due to their relevance as single-use plastics and accumulation in landfills. The chemical activation of the char was done using a strong base, KOH, that reacts with the carbonaceous structure to form pores and promote exfoliation. We focus on how the ratio of biomass to plastic can influence the final AC pore structure, surface area, and pore size in a two-step process, where char is first created and then activated. Gas analysis of the volatiles was studied using an online mass spectrometer to correlate the thermal degradation of gaseous byproducts to the formation of pores in char materials. The physicochemical and morphological properties of the char and AC were analyzed using Brunnauer–Emmett–Teller (BET) N_2 physisorption measurements, X-ray diffraction (XRD), scanning electron microscopy (SEM), Fourier-transfer infrared spectroscopy (FTIR), and X-ray photoelectron spectroscopy (XPS). Vanillin adsorption experiments were conducted to investigate the adsorptive properties of the formed AC to mimic the phenolic removal of chemical compounds in industrial wastewater streams. We discuss in detail the characteristics of the char and its influence on the adsorptive properties of the formed AC.

2. MATERIALS AND METHODS

2.1. Slow Pyrolysis and Co-pyrolysis. A Carbolite Gero Tube Furnace with a constant flow of nitrogen gas at a rate of 600 mL/min was used for the pyrolysis experiments. The feedstock comprised the corn stover, milled to 1 mm, and a plastic, either Sigma Aldrich Polystyrene MW 192 000 (1 mm beads) or hand-cut 0.5 cm squares of PET plastic from plastic water bottles. The feedstock was placed in a ceramic boat and purged with nitrogen for 5 volumes of the reactor to ensure an oxygen-free environment. The sample was then placed in the tube furnace, heated to the desired temperature at a ramp rate of 10 °C/min, held for the desired duration, and then allowed to cool to room temperature. The oil was collected using a single-pass cold trap attached to the end of the exhaust of the tube furnace. A schematic of the pyrolysis apparatus is shown in Figure S1. For the purpose of this study, the pyrolysis experiments were conducted at 500 °C for 2 h.

2.2. Chemical Activation of Char. A Thermo Scientific Type 1315M Benchtop Muffle Furnace inside a nitrogen glove box setup was used for the chemical and thermal activation of carbon. The char was combined with KOH in a 2:1 ratio of char to KOH by mass. DI water was added to the mixture and stirred for 1 h to ensure that it was homogeneous. The mixture was then dried in an oven at 105 °C overnight. The sample was transferred into the nitrogen environment muffle furnace, heated to 300 °C for 2 h at a ramp rate of 10 °C/min to remove moisture, and then further heated to 800 °C for 3 h with a ramp rate of 10 °C/min. Once cooled, the sample was washed with a 0.1 M HCl solution to neutralize any remaining KOH. The sample was vacuumed-filtered and washed with DI water until the filtrate was pH neutral. The formed AC was dried in an oven overnight at 105 °C before characterization. For the direct chemical activation method, corn stover replaced the char in equal amounts, and the rest of the procedure for chemical activation remained the same.

2.3. Thermal Degradation Pyrolysis Studies. Thermal degradative studies of the corn stover and plastic blends were studied at a heating rate of 10 °C/min from a temperature range of 50 to 500 °C in a He flow of 40 mL/min using a fixed bed reactor coupled to a Hiden quantitative gas analysis mass spectrometer. Approximately 30 mg of the CS:PET and CS:PS blends were used. Mass spectral data were obtained with an electron energy of 70 eV and an emission current of 20 μA. The signals of the selected compounds were selected after preliminary scans of the samples. The experiments performed live tracking of co-pyrolysis gaseous products, such as hydrogen (2 m/z), carbon dioxide (44 m/z), carbon monoxide (29 m/z), water (18 m/z), toluene (92 m/z), benzene (108 m/z), styrene (104 m/z), ethylene (28 m/z), and methane (16 m/z). The mass spectrometer was operated under a vacuum and detected the fragment ion and the intensity of the volatiles.

2.4. Surface Area Analysis. Surface analysis was conducted using the Micromeritics ASAP 2020 physisorption instrument to perform BET measurements. The sample was loaded and degassed for 8 h until an outgassing rate of less than 5 μm Hg/min was achieved to ensure moisture and volatile contaminants were removed before analysis. N_2 physisorption and five-point BET analysis were used to measure the surface area, pore volume, and pore size. A silica–alumina reference material with a standard error of 2.5% was used prior to experiments to assess measurement errors. Most char and AC replicates were performed to determine the intrinsic errors in the surface areas and pore sizes with 95% confidence levels.

2.5. Scanning Electron Microscopy. A TESCAN Vega3 SBH SEM was used to measure images of the various corn stover, char, and AC samples. Before imaging, the samples were placed under a vacuum, purged with argon, and then sputter-coated with Au for 10 s to improve the clarity of the images. The images were taken at 1000 times magnification with a voltage of 5 kV unless stated otherwise.

2.6. XRD and XPS. A PANalytical Empyrean Series 2 XRD instrument was utilized to evaluate the carbon structures. The emission source was Cu Kα (1.54056 A wavelength) with a Ni beta filter. A zero-diffraction plate was employed to minimize the background peaks. XPS characterization was carried out using a Kratos AXIS ULTRA XPS system equipped with an Al X-ray source and a 165 mm mean radius electron energy hemispherical analyzer. Neutralizing was done during the measurements to compensate for sample charging.

2.7. Fourier Transform Infrared Spectroscopy. Surface functional groups of char and the ACs were investigated using an FTIR Spectrometer (Nicolet 6700, Thermo Electron Corporation). The FTIR used a KBr beam splitter with a

https://doi.org/10.1021/acsomega.2c04815
ACS Omega 2023, 8, 380−390

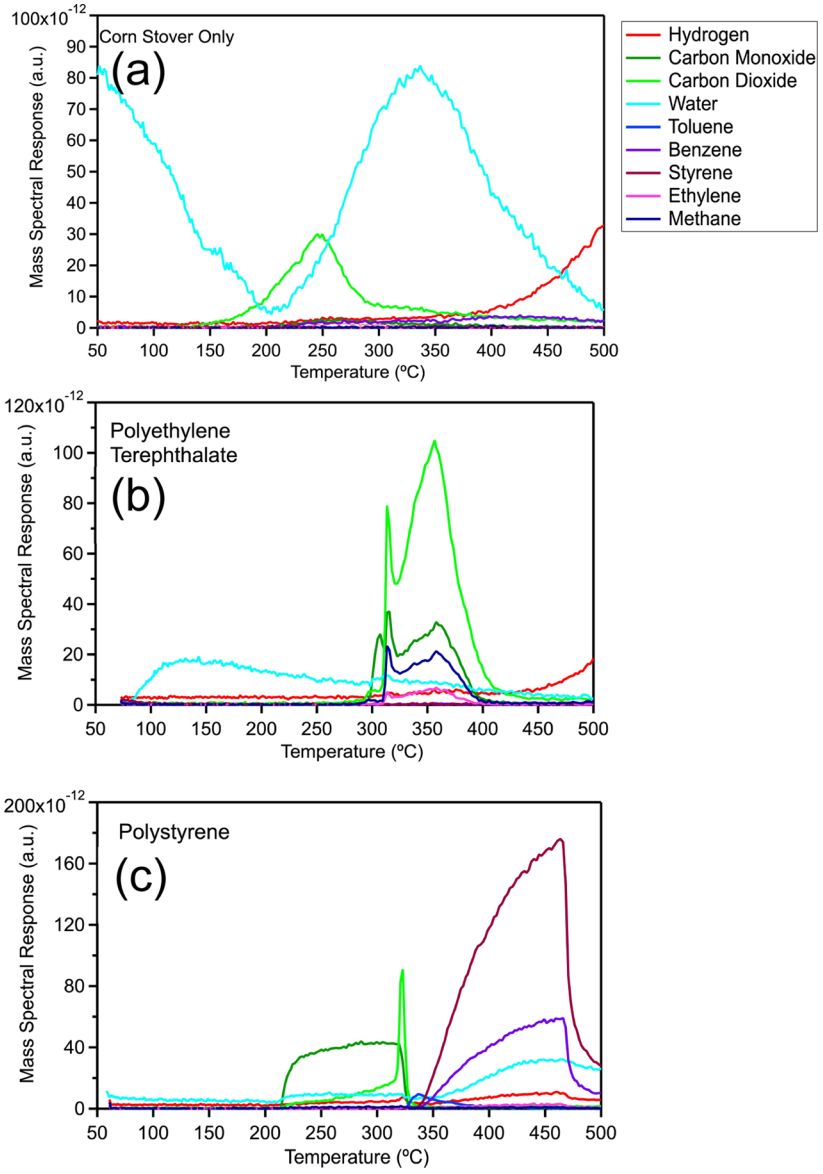

Figure 1. Live tracking analysis of the mass spectral responses of volatiles produced from (a) corn stover, (b) PET, and (c) PS during a temperature ramp to 500 °C.

deuterated triglycine sulfate detector. The gathered spectra were an average of 16 scans with 4 cm^{-1} resolution between 525−4000 cm^{-1}.

2.8. Batch Adsorption Study of Vanillin. The batch experiments of the vanillin adsorption studies using the AC and char were conducted at room temperature in a 150 mL beaker. For each run, 50 mg of the adsorbent was placed in a beaker containing 50 mL of a vanillin solution, which had a concentration of 100 mg/L. The suspension was stirred for a desired time, between 30 and 120 min, using a magnetic agitator. After agitation, the suspensions were gravity-filtered. The filtrate concentration was determined by using an Agilent Cary 60 UV−visible spectrophotometer. The absorbance wavelength was measured between 200 and 500 nm at a 60 nm/min rate and a 0.50 nm interval.

3. RESULTS AND DISCUSSION

3.1. Thermal Degradative Studies for Char Formation. The volatiles and gaseous by-products produced during thermal pyrolysis were studied for corn stover (CS), polystyrene (PS), and polyethylene terephthalate (PET) as a function of temperature and are shown in Figure 1. The thermal decomposition of corn stover occurs in two stages. The first stage involves the desorption of adsorbed water between 50 °C to 150 °C. The second stage is the main pyrolysis stage, which occurs at ∼150 °C; the most significant byproducts of pyrolysis are H_2O, CO_2, and CO. The production of H_2 at 400 °C is attributed to the continued breakdown of the solid residue formed during the temperature ramp. The initial by-products of the carbon oxides (CO_2 and CO) are most likely attributed to the breakdown of cellulose and hemicellulose, which has glucose and other sugar units with C−O fragments[25] that can occur between 200−500 °C.

The PET thermal breakdown occurs in two stages within the temperature range measured, as shown in Figure 1b. During thermal degradation, it is assumed that the polymer forms cyclic oligomers that form benzoic acid and terephthalic acid.[25] Further secondary cracking promotes the formation of gases

https://doi.org/10.1021/acsomega.2c04815
ACS Omega 2023, 8, 380−390

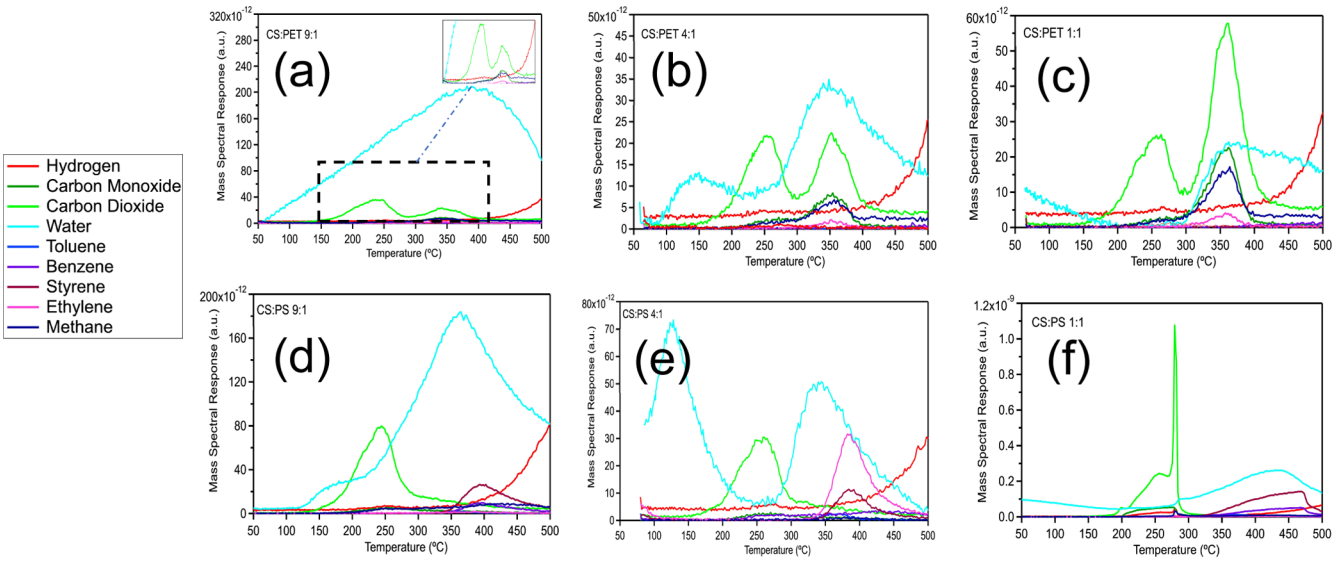

Figure 2. Thermal degradation studies of the pyrolysis of corn stover and plastics showing the main degradative gaseous products. (a) CS:PET 9:1, (b) CS:PET 4:1, (c) CS:PET 1:1, (d) CS:PS 9:1, € CS:PS 4:1, and (f) CS:PS 1:1.

(CO_2, CO, C_2H_4, CH_4, etc.) and condensable phases.[25] At temperatures above 50 °C, there is desorption of adsorbed water. The second stage is the main pyrolysis stage at ∼300 °C and starts with the generation of carbon dioxide, carbon monoxide, ethylene, benzene, and methane. The formation of CO and CO_2 is most likely attributed to the thermal decarboxylation of toluene dimethyl and benzoic acid, a byproduct of the cracking of PET.[25,26] The primary pyrolysis occurs between 410−420 °C. The generation of hydrogen at 440 °C could be attributed to the decomposition of the residual char. The thermal degradation of PS is shown in Figure 1c. PS thermal breakdown occurs in two stages. The initial stage is at 210 °C and starts with an extensive generation of carbon monoxide proceeding that of carbon dioxide, which could be attributed to either some partial oxidation of the polystyrene chain[27] or interaction of adsorbed water on the PS surface. The second stage occurs at 345 °C and is the main pyrolysis stage that produces toluene, styrene, benzene, water, and hydrogen.

Gas evolution analysis was also used to determine if the combination of plastics and corn stover had synergistic interactions, as shown in Figure 2. For the co-pyrolysis samples, water production was dominant at lower temperatures due to the desorption of adsorbed water from corn stover. In Figure 2a-c, the CS:PET 1:1 starts with the initial degradative stage at ∼175 °C with the generation of carbon dioxide; the second degradation event occurs at ∼210 °C with increased production of carbon dioxide, water, carbon monoxide, methane, and ethylene. The release of hydrogen occurs at ∼450 °C and is most likely attributed to the gasification of the formed char. CS:PET 4:1 has two breakdown stages, early outgassing of water followed by further water production at around 210 °C. The generation of CO_2 starts at 150 °C and at 210 °C with the output of CO, C_2H_4, and CH_4. CS:PET 9:1 generates the largest quantity of water for the CS:PET combined samples. Like the previous samples, there are two breakdown events with initial CO_2 production at 145 °C and 265 °C, with carbon dioxide, carbon monoxide, methane, and ethylene production. Hydrogen production occurs at around 450 °C. Figure S2a compares the carbon oxides as a function of corn stover and PET ratio. The analysis shows two primary means for generating the carbon oxides, initially from the breakdown of the biomass component at ∼210 °C and the PET at 250 °C. The largest generation of carbon oxides occurs with the lowest corn stover to plastic ratio. Interestingly, the mixture of PET decreases the onset of biomass degradation by ∼10 °C, showing an improved synergistic interaction. This corroborates previous findings by Li et al., in which the interaction of the PET-derived molecules influences the cracking behavior of cellulose.[25] The presence of water from the biomass also promotes the hydrolysis of the PET into char.[25]

Figure 2d−f shows the gas analysis for corn stover and polystyrene composites. For CS:PS 1:1, the breakdown of the composite occurs in two separate phases; at 200 °C, there is extensive production of carbon dioxide and carbon monoxide. The second production event occurs at 345 °C and initially produces toluene, followed by styrene, benzene, and hydrogen. The thermal degradation byproducts that initiate at 350 °C are attributed to the depolymerization of PS. The CS:PS 4:1 produces water initially from the desorption of water from the biomass fraction. CO_2 production initially occurs at 155 °C, and the second generation occurs at 345 °C with increased production of styrene and ethylene. The CS:PS 9:1 has an initial breakdown of biomass occurring at 150 °C with the production of CO_2; the next phase occurs at 350 °C with increased production of styrene and related byproducts. For both samples, the water generation rate is the lowest, with a higher mass ratio of plastics. The breakdown of PS occurs initially with random scission to oligomers and eventually depolymerization to yield monomers such as styrene.[28] The evolution of styrene, toluene, and benzene is attributed to the dehydration and demethylation reactions.[29]

A study by Ganesh et al. postulates that the pore size and morphology of the char formed are directly correlated to the transport and amount of volatile generated.[30] Thus, the more volatiles that diffuses out, the more pores are formed. The increase of volatiles and their rate of evolution also promote pore formation and pore dimensions. When the rate of volatile generation is high, the residence time of volatiles promotes the

https://doi.org/10.1021/acsomega.2c04815
ACS Omega 2023, 8, 380−390

formation of macro- or mesopores, which reduces the surface area and adsorbate capacity. The lower rate of char gasification produces more micropore development and a higher surface area. Thus, a higher rate of gasification would reduce the total surface area. During the carbonization of biomass and plastics, the initial stage forms residual char and promotes pore decomposition and pore formation. The volatiles from the gasification of the composite corn stover, and plastic materials can accumulate in the already developed pores, or further char gasification can open these pores or enlarge the pore dimensions.[30] The increase in volatile yield will reduce their residence time in the pores and the chances of pore blockage or condensation. The addition of plastics with corn stover should influence the char pore structure, surface area, and crystallographic structure, as discussed in section 4.

4. CHAR PROPERTIES FROM THE CO-PYROLYSIS OF CORN STOVER AND PLASTICS

4.1. Surface Area Analysis of the Formed Char. The physicochemical properties of the char from the co-pyrolysis of corn stover and polystyrene (CS:PS) and polyethylene terephthalate (CS:PET) were investigated. The surface area and pore size are crucial indicators of biomass breakdown into a carbonaceous material. Table 1 shows the surface area of neat CS and CS:PET of 1:1, 4:1, and 9:1. The ratio that formed char with the highest surface area was a CS:PET ratio of 1:1, with a value of 423.8 ± 24.2 m^2/g. The surface area of 423.8 ± 24.2 m^2/g is one of the largest measured surface areas for char, where the average char surface area is generally between 1−10 m^2/g. As the CS to PET ratio increases, the char surface area decreases, with the 4:1 and 9:1 chars having surface areas of 91.2 ± 20.4 and 74.5 ± 26.8 m^2/g, respectively. Analogously, the pore size increases as the CS to PET ratio increases from 3.0 ± 0.07 to 7.0 ± 0.71 nm. The char from neat corn stover produced a significantly lower surface area of 12.4 ± 3.7 m^2/g when compared to the CS:PET chars. The N_2 adsorption/desorption isotherms of the chars formed from corn stover and PET are shown in Figure S3d-f. The isotherms show that the formed chars have a higher adsorptive capacity as the ratio of plastics increases. The adsorptive capacity is higher than the char formed from neat corn stover (Figure S4). The material with the highest porosity is the CS:PET 1:1. Thus, a higher amount of PET impacts the CS:PET char's surface area, adsorptive capacity, pore size, and char recovery amount.[31,32] Li et al. studied the influence of volatiles in the formed chars from the co-pyrolysis and sequential pyrolysis of PET and cellulose.[25] Analogous to our findings, they determined that the PET-derived byproducts interacted with char to change the internal structures and crystallographic structure of the char. The study also determined that the cross-interaction of the volatiles produced from PET, such as the carbon oxides, further promoted the cracking reaction. We surmise that two factors influence the surface areas of the composite CS:PET chars. The addition of PET generates byproducts, such as CO_2, CO, ethylene, and benzene (as shown in Section 3), that promote unblocking of already-formed pores in the char with the added benefit of creating a microporous structure and greater surface area. Additionally, we believe that the presence of additional gases from PET-derived molecules can accelerate the breakdown of cellulose and hemicellulose, resulting in a char with more lignin content than that formed from neat corn stover. As lignin-rich biomass tends to have higher porosity and surface area,[33] we believe the improved surface area of the char is attributed to the increase in volatile transport and formed char with higher lignin component.

The ratio of CS to PS was varied from 1:1, 4:1, and 9:1 to investigate the impact of the addition of PS on the properties of the char formed. Table 1 shows that the addition of PS has a nominal change in the composite surface area. The highest surface area of the chars containing PS was the 4:1 ratio at 11.7 ± 2.8 m^2/g. Generally, the measured pore sizes for the CS:PS chars were higher than the control sample, where the CS:PS 1:1 sample achieved a pore size of 32.2 ± 2.7 compared to the control neat CS of 12.3 ± 10.6 nm. The N_2 adsorption/

Table 1. Surface Area of Char as a Function of the Mass Ratio of Corn Stover and Plastics (CS:PET and CS:PS Ratio)

	sample CS-PS (2 h, 500 °C)	surface area (m^2/g)	BJH pore size (nm)	% recovered as a function of corn stover
CS-PS	1:1 ratio	6.5 ± 0.8	32.2 ± 2.7	31.3%
	4:1 ratio	11.7 ± 2.8	19.6 ± 14.1	32.2%
	9:1 ratio	7.0 ± 3.2	22.3 ± 7.5	31.7%
CS-PET	1:1 ratio	423.8 ± 24.2	3.0 ± 0.07	53.2%
	4:1 ratio	91.2 ± 20.4	5.2 ± 0.57	39.3%
	9:1 ratio	74.5 ± 26.8	7.0 ± 0.71	36.1%
neat CS	1:0 ratio	12.4 ± 3.7	12.3 ± 10.6	32.4%

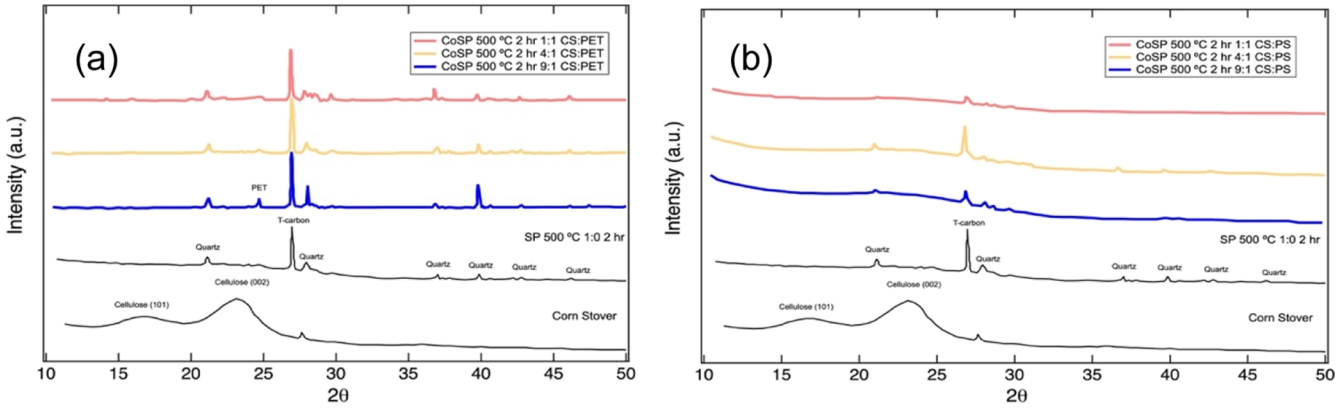

Figure 3. XRD spectra of the chars produced from the co-pyrolysis of (a) CS:PET and (b) CS:PS as a function of the ratio of corn stover to plastics. The spectra are compared to untreated corn stover and char control sample from corn stover (denoted as SP 500 °C).

https://doi.org/10.1021/acsomega.2c04815
ACS Omega 2023, 8, 380−390

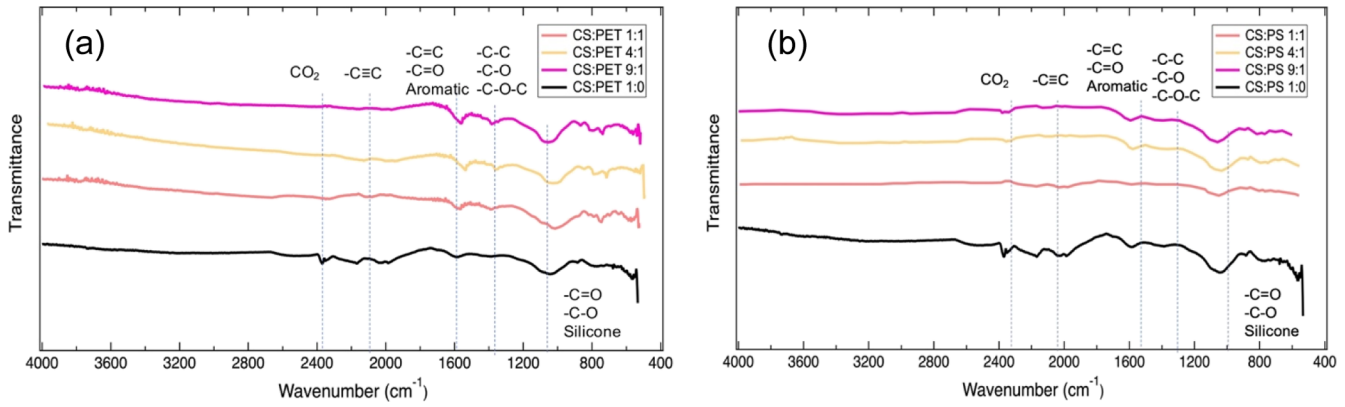

Figure 4. Fourier-transform infrared spectra of (a) CS:PET and (b) CS:PS as a function of the ratio of corn stover to plastics.

desorption isotherms of the chars formed from corn stover and PS are shown in Figure S2a−c. The isotherms show that the formed chars have a slightly higher adsorptive capacity as the ratio of plastics is increased. The adsorptive capacity is lower compared to the char formed from corn stover only. The material with the highest adsorptive capacity is the CS:PS 1:1. The trend suggests that PS synergistically promotes the formation of larger pores in the char and a smaller surface area with minimal changes in the adsorptive capacity. This is corroborated by a similar study from Özsin et al. on the co-pyrolysis of biomass and polystyrene. Their team posited that the char formed during co-pyrolysis had a porous structure due to the increased diffusion rate of the evolved gases produced.[29] The CS:PS chars had lower surface areas but larger average pore sizes than the control neat CS samples. Based on the experiments and gas evolution analysis, we surmise that the thermal degradation breakdown of PS increases the residence time of formed volatiles in the pores of the char, increasing the relative size and lower surface area. The results indicate that the formed char comprises mainly carbonaceous species from corn stover and that the PS mass plays little to no part in the recovery amount of the formed char. This was also confirmed in thermal degradation studies, where the char formed from PS was negligible when compared to PET and CS. The pyrolysis of PS with corn stover promotes the porosity of the lignocellulosic content promoting the transport of the formed volatiles and interactions of radicals occurring during degradation.[29]

4.2. Composition and Crystallinity Analysis Using XRD. Figure 3 shows the XRD spectra of the chars produced from slow pyrolysis of CS:PS or PET. The XRD spectra show the transformation of the composite corn stover and plastic materials to the carbonaceous structure of the formed chars. Figure 3a shows the XRD of char formed from the co-pyrolysis of CS mixed with PET compared to char formed from the pyrolysis of neat corn stover at 500 °C. The 4:1 and 1:1 CS:PET ratios show increased turbostatic or t-carbon peaks at 26.6° 2θ. We surmise that the addition of PET promotes the breakdown of the CS biomass and the formation of the t-carbon graphitic layers increasing the surface area, as reflected in the surface area measurements shown in Table 1. However, the addition of PET also seems to influence the quartz peak, which overlaps with the PET diffraction peaks at 27 and 29 2θ.[25] The appearance of new peaks at 27 and 29 2θ with a higher mass fraction of PET confirms that some residual PET remains on the surface after the formation of char.[25] The peak at 20.6−21.2°, ∼27, ∼36, ∼44, and ∼47 2θ coincides with quartz carbon.[34−36] When comparing the char XRD spectra from CS only to that of chars from CS-PET, there are more pronounced peaks of crystalline quartz carbon. The crystalline quartz peaks decrease in intensity with further addition of plastic. All CS:PET ratios show a peak at 24.3° 2θ, which is a peak reflective of PET.[36] The XRD spectra indicate that there is residual PET on the surface of the char at detectable levels after pyrolysis at 500 °C. PET degradation produces acids and oligomers that promote the breakdown of the char and form more t-carbon species. The PET degradation compounds may condense in the pores of the char forming small granules.

Figure 3b shows the XRD spectra of the chars produced from the co-pyrolysis of CS:PS. The CS:PS char spectra show the formation of turbo-static carbon but have a minimal formation of quartz carbon. There are no detectable levels of polystyrene on the char surface, which confirms the complete breakdown of polystyrene during the pyrolysis experiments. This corroborates prior studies that indicate PS contributes to minimal char formation and generally breakdown into a liquid and gas fraction.[16] As the mass ratio of CS:PS decreases, there is less prevalence of t-carbon. For instance, the 1:1 ratio of CS-PS char has less intense t-carbon and quartz carbon peaks than the 4:1 ratio of CS char. The trend suggests that PS influences the carbonization process and may suppress the formation of exfoliated layers (t-carbon).

4.3. Analysis of Functional Groups. FTIR was used to assess the surface functional groups on the formed chars. The FTIR of CS-PET char as a function of the CS:PET ratio is shown in Figure 4a. The FTIR spectra show that for all corn stover and PET samples, there is stretching in the double bond region attributed to C═O and C═C. An additional peak is observed around 1400 cm^{-1}, indicating C−C, C−O−C, and C−O bonds. The FTIR spectra of the CS:PET as a function of the mass ratio do not differ much. However, it does appear that there is more prominence of the unsaturated carbon species as the amount of PET increases. The C═O and C−O stretchings are observed on all the char around 880−1200 cm^{-1}. The FTIR also showed a potential residue PET polymer peak around 1400 cm^{-1}. The addition of PET promotes more aromatic surface functional groups in the char formed.

The FTIR of the CS-PS chars can be seen in Figure 4b. The chars of CS and CS-PS show some triple bond stretching around 2100 cm^{-1} (C≡C). There is stretching in the double bond region around 1530−1610 cm^{-1} which is attributed to C═O and C═C. The CS:PS 4:1 char has a more intense peak

https://doi.org/10.1021/acsomega.2c04815
ACS Omega 2023, 8, 380−390

in the double bond region, whereas the char CS and CS:PS 1:1 have shallower peaks. The stretching of C−O and C═O from alcohols, carbonyl groups, and potentially silicone can be observed from 860−1200 cm^{-1}. As with PET, adding polystyrene to CS:PS increases the amount of aromatics and C═O functional groups in the formed solid product char. The source of the additional aromatic groups is most likely the styrene (PS) or terephthalic acid monomeric groups that form after the degradation of the synthetic polymer chains of the plastics.

4.4. Morphological Analysis of Char Using SEM. Select SEM images of the CS:PET chars are shown in Figure 5.

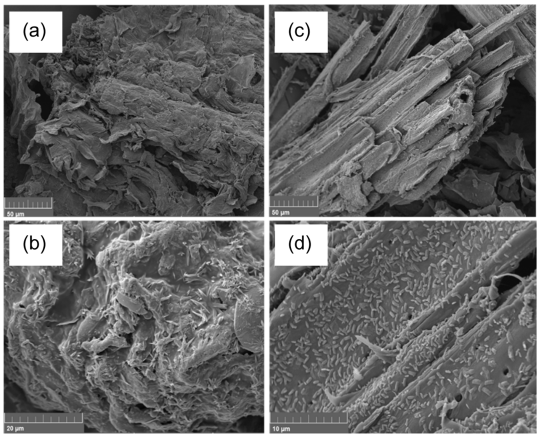

Figure 5. Select images of char formed from the pyrolysis of CS:PET at 500 °C for 2 h (a) CS:PET 1:1 1 kx, (b) CS:PET 1:1 4.2kx, (c) CS:PET 9:1 1kx, and (d) CS:PET 9:1 8kx.

Figure 5 shows the SEM imaging of the PET char as a function of the CS:PET ratio. The images show the CS:PET ratios with the highest (CS:PET 1:1) and lowest (CS:PET 9:1) PET amounts. As can be seen from Figure 5b,d, there are noticeable grain-like deposits on the char surface for both the CS:PET ratios of 1:1 and 9:1, respectively. The grain-like rice deposits are not shown in the SEM imaging of the control neat CS samples shown in Figure S5. We postulate that the grain-like deposits shown in Figure 5b could be the formation of condensed PET oligomers on the surface identified earlier by XRD. The CS:PET 9:1 char shows wood-like structures and less degradation of the carbide structure. The breakdown of the char differences is attributed to the content of plastic and biomass within the reactor. For instance, the CS:PET 9:1 has 80% more corn stover than the 1:1 ratio, which partially accounts for the drastic difference in the appearance of the char. The SEM images for CS-PS are shown in Figure 6. The various ratios show no observable degradation or morphological differences in the samples as a function of the mass ratio. The CS:PS char resembles that of the char produced from CS (Figure S5), and the wood-like structure of corn stover is still visible. Compared to corn stover mixed with PET, we surmise that the addition of PS to corn stover during co-pyrolysis has minimal changes in the morphological properties of the composite char.

4.5. AC Properties from Co-pyrolysis of Corn Stover and Plastic. *4.5.1. Physicochemical Properties of AC from CS and PET.* The chars formed from the co-pyrolysis of corn stover and plastics were chemically activated using potassium hydroxide to produce AC. The properties of the ACs were characterized using XRD, FTIR, XPS, and SEM and compared to that of AC formed from the chemical activation of char-derived corn stover. Finally, we probed the adsorptive properties of the AC to remove a phenolic compound, vanillin. The adsorptive properties indirectly measure how effective the available surface functional groups are in removing phenols from simulated wastewater.

For AC derived from CS:PS, the material with the highest surface area (430.3 ± 15.6 m^2/g) was obtained from the char precursor formed from a CS:PS ratio of 4:1. There does not seem to be a noticeable trend in how the CS:PS ratio influences the surface area or pore size. The average surface area for all ACs formed from the char precursors from CS:PS is 437 m^2/g. The AC surface area for CS:PS composite materials is considerably lower than that of the AC formed from corn stover-only char precursors, as can be seen in Table 2. The N_2 adsorption/desorption isotherms of the AC formed from corn stover and PS are shown in Figure S6a-c. The isotherms show that all the formed AC have a similar adsorptive capacity for all ratios studied. The adsorptive capacity is lower when compared to the AC formed from neat corn stover (Figure S7). For AC derived from CS:PET, the material with the highest surface area, was AC CS:PET 1:1, with a value of 409.2 ± 1.2 m^2/g. The surface area of AC CS:PET 4:1 had a measured surface area of 373.1 m^2/g. The obtained AC CS:PET 4:1 surface area is also the lowest for all ACs derived

Table 2. Surface Area of Activated Carbon as a Function of the Temperature and Char Composition

sample	surface area (m^2/g)	pore size (nm)
AC CS:PS 1:1	430.3 ± 15.6	4.2 ± 0.09
AC CS:PS 4:1	477.0 ± 40.8	4.1 ± 0.04
AC CS:PS 9:1	404.7 ± 5.7	4.7 ± 0.09
AC CS:PET 1:1	409.2 ± 1.2	4.6 ± 0.01
AC CS:PET 4:1	373.1 ± 17.1	8.5 ± 0.29
AC CS:PET 9:1	390.1 ± 10.7	4.8 ± 0.25
AC from neat CS	614.4 ± 0.2	3.9 ± 0.19

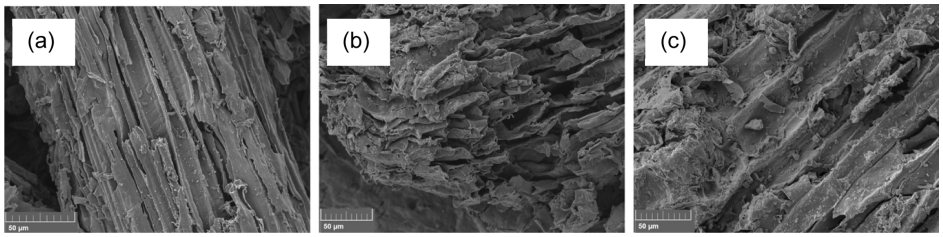

Figure 6. Select images of char formed from the pyrolysis of CS:PS at 500 °C for 2 h (a) CS:PS 1:1 1.2 kx, (b) CS:PS 4:1 0.95kx, and (c) CS:PS 9:1 1.0kx.

https://doi.org/10.1021/acsomega.2c04815
ACS Omega 2023, 8, 380−390

from the CS:plastic composite materials. The average surface area for all ACs formed from CS:PET is 390.8 m^2/g. The N_2 adsorption/desorption isotherms of the AC formed from corn stover and PET are shown in Figure S6d−f. The isotherms show that all of the formed AC have a similar adsorptive capacity for all ratios studied. The adsorptive capacity is lower when compared to the AC formed from neat corn stover (Figure S7). It appears that the addition of PET is detrimental to the final surface area produced for the Acs. We postulate that the addition of plastics modifies the crystallographic structure of the char formed, limiting the efficacy of chemical activation by KOH. As postulated earlier, the addition of PET and PS promotes the lignocellulosic cracking reactions forming chars with high surface areas and high lignin contents. In our previous article on the slow pyrolysis of corn stover,[37] we discussed chars with higher lignin concentration tend to have lower surface areas, where the aromatic backbone is more prone to produce macropores.[37] Thus, the addition of plastics may be prohibitory to the surface area and porosity of the formed AC.

4.5.2. Composition and Crystallinity of Activated Carbon Using XRD and XPS. Figure 7 shows the XRD results for the AC from the CS:plastic composites. The XRD spectra for all AC CS:PET, shown in Figure 7a, show broad, amorphous peaks. However, as the ratio of CS:PET increases, turbo-static and quartz carbon's crystallographic peaks become more prominent and then decrease. For example, the AC CS:PET 1:1 peaks show amorphous peaks; as the amount of corn stover increases, graphitic and quartz carbon peaks are formed. The XRD results for all AC CS:PS samples studied are shown in Figure 7b and show amorphous peaks. Like AC CS:PET, AC CS:PS shows pronounced crystallinity with turbo-static and quartz carbon peaks for all samples. The AC derived from the corn-stover char precursors is completely amorphized. The XRD spectra confirm that the presence of the plastics in the char precursors influences the carbonaceous structure of the formed ACs compared to the control AC sample.

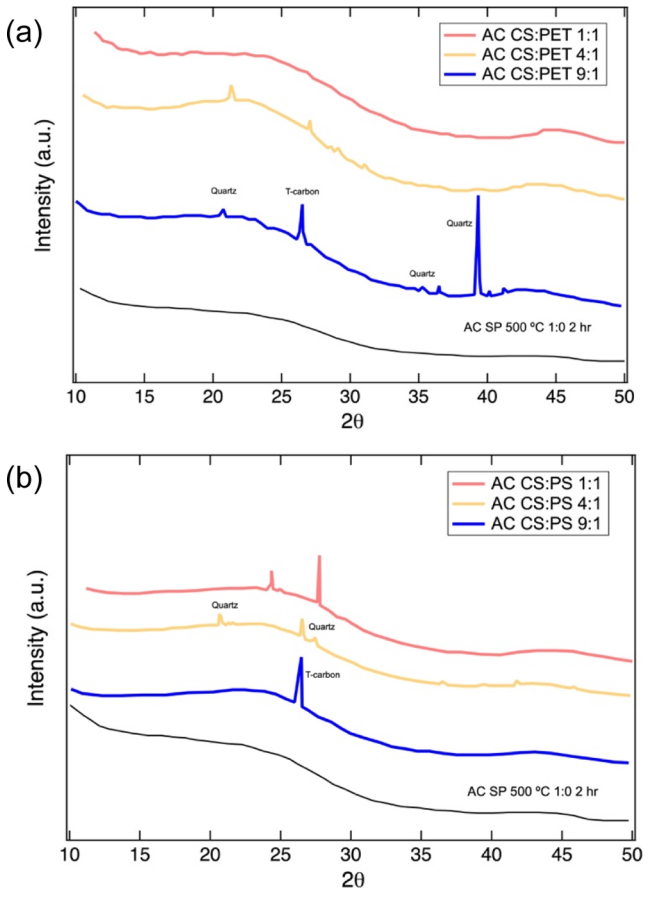

Figure 7. XRD spectra of AC samples derived from CS:plastic char precursors as a function of the mass ratio, (a) ACs from corn stover and polyethylene terephthalate (AC CS:PET), and (b) ACs from corn stover and polystyrene (AC CS:PS). The spectra are compared to the AC control sample derived from corn stover char (denoted as AC SP 500 °C).

The elemental analysis for the CS:Plastic 1:1 composite chars and related ACs was conducted using XPS, as shown in Table S1. The CS-PET 1:1 created the lowest oxygen-containing char at 15%. The presence of acids can contribute to the acidic dehydration of cellulose, decreasing the O atoms of the lignocellulosic content. After chemical activation, the oxygen content increased to 23%, the lowest of the formed CS:Plastic ACs. For all AC measurements, the O/C ratio increased. For example, the activation of char-derived from corn stover only had a minor jump in oxygen content, from 21 to 24%, while AC CS:PS 1:1 had a more significant jump, from 18 to 26%. AC CS-PET had the lowest surface areas and had comparatively lower oxygen chars. The CS:PET and CS:PS char samples have the lowest oxygen content compared to the char derived from corn stover-only samples. A prior study by Chen et al. determined the propensity of the activation of chars and the introduction of O-containing as a function of the amount of KOH added.[38] We postulate that the presence of plastics in the corn stover residue promotes additional side reactions that produce either excess hydrogen or acids that cause deoxygenation of the char.

4.5.3. Morphological Properties and the Associated Surface Functional Groups for the ACs. The adsorption characteristics of the AC formed from the CS:Plastic composites depend on the surface functional groups. FTIR analysis was used to analyze the surface functional groups of the ACs as a function of the compositions. Figure 8 shows the FTIR results of the AC CS-PET and AC CS-PS ACs. The peaks for all the AC are similar. The AC FTIR spectra have slightly different stretching intensities for adsorbed CO_2 and carbon triple bonds and a broad peak for the C−O and C−O−C stretches. Compared to the char's prominent surface functional groups, there are few prominent peaks for AC corresponding to C═C, and many of the peaks disappear in the fingerprint region. For AC CS:PETs for all ratios, there is also no peak around 1400 cm^{-1}, which may be credited to the breakdown of the PET after chemical activation in strongly alkaline conditions.

Figure 9 shows the SEM images of select AC samples formed from CS:PET or CS:PS-derived chars. The AC CS:PS images show differences in surface structure and course appearance. The AC CS:PS peaks also have clearly defined pores and do not show any real changes in the morphology for all mass ratios. In comparison, the AC CS:PET shows the formation of the pores, which become more prevalent at a mass ratio of 9:1. This may corroborate our analysis of the surface area and XRD spectra that the higher the biomass content of the char, the higher the propensity to activate the structure. A close inspection of the surfaces at higher magnification also does not see any granule structures, which confirms the breakdown of the PET granules condensed on the

https://doi.org/10.1021/acsomega.2c04815
ACS Omega 2023, 8, 380−390

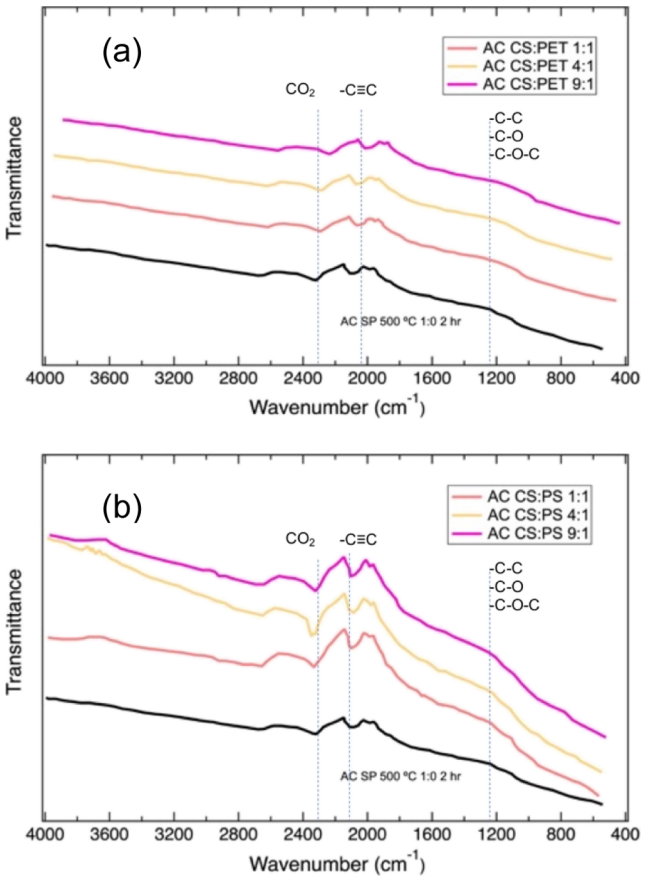

Figure 8. Fourier-Transform Infrared spectra of AC from (a) corn stover and polyethylene terephthalate (AC CS:PET) and (b) corn stover and polystyrene (AC CS:PS) as a function of the ratio of corn stover to plastics.

surface. This is expected as the high temperatures used for chemical activation promote the thermal degradation of the PET completely in an environment of strong alkaline conditions. In summary, the characteristics (prevalent functional groups, surface area, and morphology) of AC CS:PS and AC CS:PET are similar.

4.5.4. Adsorbent Properties of ACs for Vanillin. The adsorption characteristics of the porous carbon formed from CS:Plastic composites depend on the prominent surface functional groups. Although the FTIR spectroscopy results show that all ACs have similar surface structures, the vanillin adsorption experiments indirectly measure the propensity of the porous carbons and ACs to adsorb pollutant species from water. Figure 10 shows the AC CS removed 95% of the vanillin (100 mg/L) after 2 h. AC CS-PS and AC CS-PET removed 45 and 46%, respectively, after 2 h. The porous char from CS:PET 1:1 had negligible removal efficiency. The AC from CS-PS and CS-PET performed almost identically for all the trials. AC derived from CS outperformed the other ACs significantly across all tested durations. Although the higher surface area of AC CS played a role in better adsorption, we postulate that the improved adsorbate capacity could be due to the number of adsorption sites, surface functional groups, and pore sizes. The detrimental performance of the CS:PET 1:1 char could be attributed to the limited pore size prohibiting the adsorption of vanillin and the insufficient concentration of oxygen functional groups to promote physisorption. This is confirmed with XPS analysis of the O/C ratio (Table S1), which shows that CS-PET char has the lowest O/C concentration among all chars and AC measured. We calculated the adsorbate capacity normalized to the surface area to corroborate this theory. Although AC CS:PS has a marginally higher surface area than AC CS:PET, the performance of both ACs derived from corn stover and plastic composites is about the same. The presence of the plastics in the char precursor produced an AC with inferior properties to adsorb vanillin additives. We surmise that this is attributed to the ineffective activation of the corn stover.

5. CONCLUSIONS

The physicochemical properties of char and AC produced from the co-pyrolysis of corn stover and plastic (PS or PET) were evaluated. The findings suggest that plastics synergistically affect the formation of chars with either larger pore sizes or larger surface areas. Gas analysis suggests that the evolution of gas byproducts from the cracking of synthetic and natural polymers can influence the char crystallographic structure, pore structure, pore size, and surface area. The AC produced from CS:PS and CS:PET had lower O/C composition, lower surface

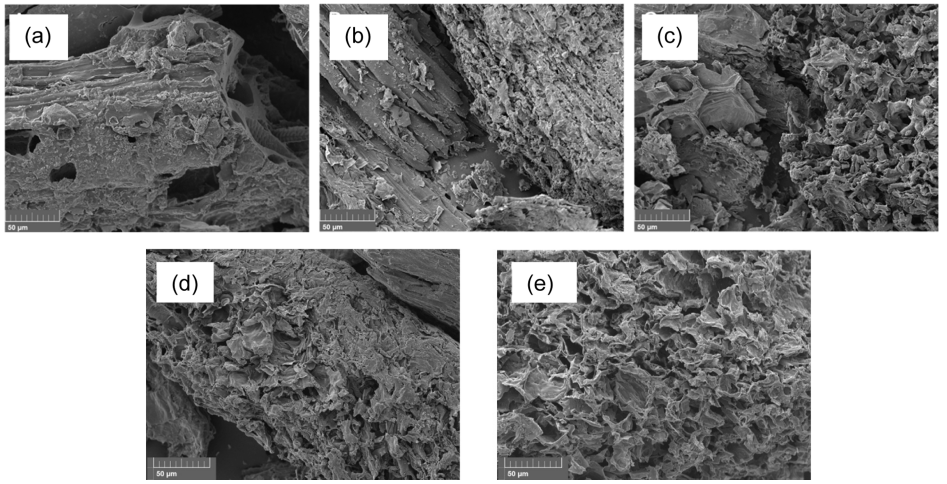

Figure 9. SEM images of select AC samples as a function of the char obtained from the pyrolysis of CS and plastics in various mass ratios. (a) AC from CS:PET 1:1, (b) AC from CS:PET 4:1, (c) AC from CS:PET 9:1, (d) AC from CS:PS 4:1, and (e) AC from CS:PS 9:1.

https://doi.org/10.1021/acsomega.2c04815
ACS Omega 2023, 8, 380−390

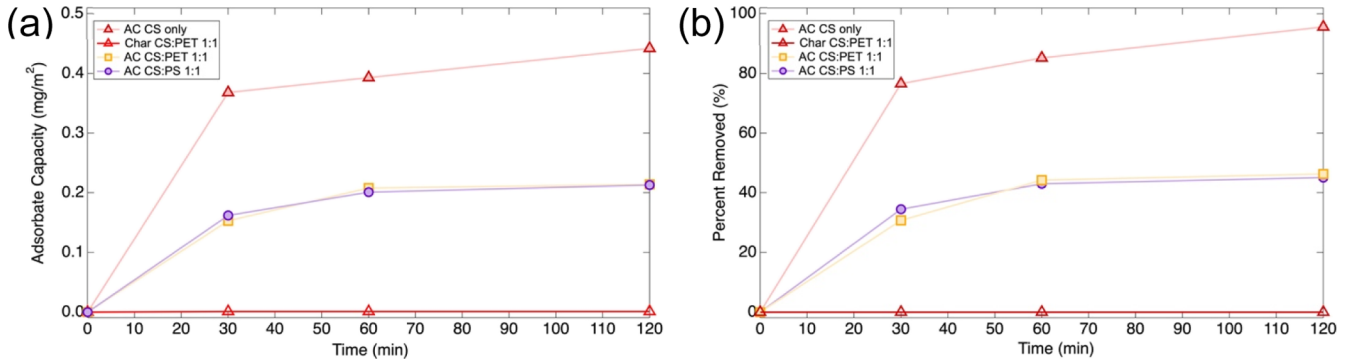

Figure 10. (a) Vanillin adsorbate capacity normalized to the surface area of the ACs as a function of time. (b) Percentage of Vanillin removal as a function of time.

areas, and higher crystallinity than AC derived from corn stover char. During co-pyrolysis, the breakdown of the plastics promotes additional side reactions (production of carbon oxides, methane, ethylene, etc.) that change the crystallographic properties, porosity, and prevalent surface functional groups of both the char and AC. The chars from CS:PET 1:1 had the highest measured surface area at a 1:1 ratio, 423.8 ± 24.8 m^2/g. Adding PS to the corn stover promoted char formation, with an average larger pore size and smaller surface area. The corn stover and polystyrene char and ACs had no evidence of plastics in the residual carbonaceous products. All the ACs formed from corn stover/plastics performed inferior to the corn stover char-derived samples. This finding shows that the properties of co-pyrolysis char can be influenced by the interaction between the plastic and the biomass during the process. The addition of plastics promotes side reactions that produce hydrogen or acids, contributing to a higher yield of the formed solid residue char. The alteration of the surface, porosity, and crystallographic structure due to the presence of the polymers may have an antagonistic effect on the properties of the chars as precursors for AC.

■ ASSOCIATED CONTENT

Supporting Information

The Supporting Information is available free of charge at https://pubs.acs.org/doi/10.1021/acsomega.2c04815.

Schematic of the pyrolysis reactor, images of char from corn stover, BET isotherms for char and AC formed from corn stover and plastic mixtures, elemental analysis of select char and AC, and thermal degradation analysis monitoring of carbon oxides of CS:PET and CS:PS (PDF)

■ AUTHOR INFORMATION

Corresponding Author

Kandis Leslie Gilliard-AbdulAziz − *Department of Chemical and Environmental Engineering, Bourns College of Engineering and Department of Material Science and Engineering, Bourns College of Engineering, University of California, Riverside, Riverside, California 92521, United States;* orcid.org/0000-0002-1706-9552; Phone: (951) 827-9158; Email: klabdulaziz@engr.ucr.edu

Authors

Mark Gale − *Department of Chemical and Environmental Engineering, Bourns College of Engineering, University of California, Riverside, Riverside, California 92521, United States;* orcid.org/0000-0002-4740-5860

Peter M. Nguyen − *Department of Material Science and Engineering, Bourns College of Engineering, University of California, Riverside, Riverside, California 92521, United States*

Complete contact information is available at: https://pubs.acs.org/10.1021/acsomega.2c04815

Notes

The authors declare no competing financial interest.

■ ACKNOWLEDGMENTS

The authors would like to thank Dr. Charles Wyman and Dr. Charles M. Cai for providing the corn stover for the experiments. The authors thank Dr. Ilkeun Lee for his XPS analytical support. We would also like to acknowledge the Analytical Chemistry Instrumentation Facility at the University of California, Riverside, for supporting UV Vis and FTIR spectroscopy. The authors would like to acknowledge the University of California, Riverside, for the financial support. P.M.N. graciously acknowledges the financial support from the University of California's Leadership Excellence through the Advanced Degree (UC LEADS) program, which prepares promising students for advanced education in science, technology, mathematics, and engineering (STEM).

■ REFERENCES

(1) Chamas, A.; Moon, H.; Zheng, J.; Qiu, Y.; Tabassum, T.; Jang, J. H.; Abu-Omar, M.; Scott, S. L.; Suh, S. Degradation Rates of Plastics in the Environment. *ACS Sustain. Chem. Eng.* **2020**, *8*, 3494−3511.
(2) Gibb, B. C. Plastics Are Forever. *Nat. Chem.* **2019**, *11*, 394−395.
(3) Yoshida, S.; Hiraga, K.; Takehana, T.; Taniguchi, I.; Yamaji, H.; Maeda, Y.; Toyohara, K.; Miyamoto, K.; Kimura, Y.; Oda, K. A Bacterium That Degrades and Assimilates Poly(Ethylene Terephthalate). *Science 80* **2016**, *351*, 1196−1199.
(4) Müller, R. J.; Kleeberg, I.; Deckwer, W. D. Biodegradation of Polyesters Containing Aromatic Constituents. *J. Biotechnol.* **2001**, *86*, 87−95.
(5) Danso, D.; Chow, J.; Streit, W. R. Plastics: Environmental and Biotechnological Perspectives on Microbial Degradation. *Appl. Environ. Microbiol.* **2019**, *85*(). DOI: 10.1128/AEM.01095-19.
(6) Ho, B. T.; Roberts, T. K.; Lucas, S. An Overview on Biodegradation of Polystyrene and Modified Polystyrene: The Microbial Approach. *Crit. Rev. Biotechnol.* **2018**, *38*, 308−320.
(7) Celik, G.; Kennedy, R. M.; Hackler, R. A.; Ferrandon, M.; Tennakoon, A.; Patnaik, S.; LaPointe, A. M.; Ammal, S. C.; Heyden,

A.; Perras, F. A.; et al. Upcycling Single-Use Polyethylene into High-Quality Liquid Products. *ACS Cent. Sci.* **2019**, *5*, 1795−1803.
(8) Zhuo, C.; Levendis, Y. A. Upcycling Waste Plastics into Carbon Nanomaterials: A Review. *J. Appl. Polym. Sci.* **2014**, *131*, a−n.
(9) Allred, R. E.; Busselle, L. D. Tertiary Recycling of Automative Plastics and Composites. *J. Thermoplast. Compos. Mater.* **2000**, *13*, 92−101.
(10) Rutkowski, P. Influence of Zinc Chloride Addition on the Chemical Structure of Bio-Oil Obtained during Co-Pyrolysis of Wood/Synthetic Polymer Blends. *Waste Manag.* **2009**, *29*, 2983−2993.
(11) Rutkowski, P.; Kubacki, A. Influence of Polystyrene Addition to Cellulose on Chemical Structure and Properties of Bio-Oil Obtained during Pyrolysis. *Energy Convers. Manag.* **2006**, *47*, 716−731.
(12) Abnisa, F.; Daud, W. M. . W.; Sahu, J. N. Pyrolysis of Mixtures of Palm Shell and Polystyrene: An Optional Method to Produce a High-Grade of Pyrolysis Oil. *Environ. Prog. Sustain. Energy* **2014**, *33*, 1026−1033.
(13) Libra, J. A.; Ro, K. S.; Kammann, C.; Funke, A.; Berge, N. D.; Neubauer, Y.; Titirici, M. M.; Fühner, C.; Bens, J.; Kern, K. H.; Emmerich, K.-H. Hydrothermal Carbonization of Biomass Residuals: A Comparative Review of the Chemistry, Processes and Applications of Wet and Dry Pyrolysis. *Biofuels* **2011**, *2*, 71−106.
(14) Sharypov, V. I.; Beregovtsova, N. G.; Kuznetsov, B. N.; Cebolla, V. L.; Collura, S.; Finqueneisel, G.; Zimny, T.; Weber, J. V. Influence of Reaction Parameters on Brown Coal-Polyolefinic Plastic Co-Pyrolysis Behavior. *J. Anal. Appl. Pyrolysis* **2007**, *78*, 257−264.
(15) Wang, J.; Jiang, J.; Wang, X.; Wang, R.; Wang, K.; Pang, S.; Zhong, Z.; Sun, Y.; Ruan, R.; Ragauskas, A. J. Converting Polycarbonate and Polystyrene Plastic Wastes Intoaromatic Hydrocarbons via Catalytic Fast Co-Pyrolysis. *J. Hazard. Mater.* **2020**, *386*, 121970.
(16) Özsin, G.; Pütün, A. E. A Comparative Study on Co-Pyrolysis of Lignocellulosic Biomass with Polyethylene Terephthalate, Polystyrene, and Polyvinyl Chloride: Synergistic Effects and Product Characteristics. *J. Clean. Prod.* **2018**, *205*, 1127−1138.
(17) Önal, E.; Uzun, B. B.; Pütün, A. E. Bio-Oil Production via Co-Pyrolysis of Almond Shell as Biomass and High Density Polyethylene. *Energy Convers. Manag.* **2014**, *78*, 704−710.
(18) Abnisa, F.; Wan Daud, W. M. A. A Review on Co-Pyrolysis of Biomass: An Optional Technique to Obtain a High-Grade Pyrolysis Oil. *Energy Convers. Manag.* **2014**, *87*, 71−85.
(19) Velten, S.; Boller, M.; Köster, O.; Helbing, J.; Weilenmann, H.; Hammes, F. Development of biomass in a drinking water granular active carbon (GAC) filter. *Water Res.* **2011**, *45*, 6347−6354.
(20) Spahis, N.; Addoun, A.; Mahmoudi, H.; Ghaffour, N. Purification of Water by Activated Carbon Prepared from Olive Stones. *Desalination* **2008**, *222*, 519−527.
(21) Abumaizar, R. J.; Kocher, W. M.; Smith, E. H. Biofiltration of BTEX contaminated air streams using compost-activated carbon filter media. *J. Hazard. Mater.* **1998**, *60*, 111−126.
(22) Yang, S.; Zhu, Z.; Wei, F.; Yang, X. Carbon nanotubes / activated carbon fiber based air filter media for simultaneous removal of particulate matter and ozone. *Build. Environ.* **2017**, *125*, 60−66.
(23) Dimitratos, N.; Villa, A.; Prati, L. Liquid Phase Oxidation of Glycerol Using a Single Phase (Au-Pd) Alloy Supported on Activated Carbon: Effect of Reaction Conditions. *Catal. Lett.* **2009**, *133*, 334−340.
(24) Jung, K. B.; Lee, J.; Ha, J. M.; Lee, H.; Suh, D. J.; Jun, C. H.; Jae, J. Effective Hydrodeoxygenation of Lignin-Derived Phenols Using Bimetallic RuRe Catalysts: Effect of Carbon Supports. *Catal. Today* **2018**, *303*, 191−199.
(25) Li, C.; Sun, Y.; Li, Q.; Zhang, L.; Zhang, S.; Wang, H.; Hu, G.; Hu, X. Effects of Volatiles on Properties of Char during Sequential Pyrolysis of PET and Cellulose. *Renewable Energy* **2022**, *189*, 139−151.
(26) Li, C.; Ataei, F.; Atashi, F.; Hu, X.; Gholizadeh, M. Catalytic Pyrolysis of Polyethylene Terephthalate over Zeolite Catalyst: Characteristics of Coke and the Products. *Int. J. Energy Res.* **2021**, *45*, 19028−19042.
(27) Yousif, E.; Haddad, R. Photodegradation and Photostabilization of Polymers, Especially Polystyrene: Review. *Springerplus* **2013**, *2*, 398.
(28) Ahmad, Z.; Al-Sagheer, F.; Al-Awadi, N. A. Pyro-GC/MS and thermal degradation studies in polystyrene-poly(vinyl chloride) blends. *J. Anal. Appl. Pyrolysis* **2010**, *87*, 99−107.
(29) Özsin, G.; Pütün, A. E. Insights into Pyrolysis and Co-Pyrolysis of Biomass and Polystyrene: Thermochemical Behaviors, Kinetics and Evolved Gas Analysis. *Energy Convers. Manag.* **2017**, *149*, 675−685.
(30) Raveendran, K. Adsorption Characteristics and Pore-Development of Biomass-Pyrolysis Char. *Fuel* **1998**, *77*, 769−781.
(31) Buxbaum, B. Y. L. H. The Degradation of Poly(ethylene terephthalate). *Angew. Chem., Int. Ed.* **1968**, *7*, 182−190.
(32) Dimitrov, N.; Kratofil Krehula, L.; Ptiček Siročić, A.; Hrnjak-Murgić, Z. Analysis of Recycled PET Bottles Products by Pyrolysis-Gas Chromatography. *Polym. Degrad. Stab.* **2013**, *98*, 972−979.
(33) Zhang, N.; Shen, Y. One-Step Pyrolysis of Lignin and Polyvinyl Chloride for Synthesis of Porous Carbon and Its Application for Toluene Sorption. *Bioresour. Technol.* **2019**, *284*, 325−332.
(34) Melo, D. M. A.; Ruiz, J. A. C.; Melo, M. A. F.; Sobrinho, E. V.; Schmall, M. Preparation and Characterization of Terbium Palygorskite Clay as Acid Catalyst. *Microporous Mesoporous Mater.* **2000**, *38*, 345−349.
(35) Xiao, W.; Han, L.; Zhao, Y. Comparative Study of Conventional and Microwave-Assisted Liquefaction of Corn Stover in Ethylene Glycol. *Ind. Crops Prod.* **2011**, *34*, 1602−1606.
(36) Kevin Eiogu, I.; Ibeneme, U.; Aiyejagbara, O. M. Identification of Polyethylene Terephthalate (PET) Polymer Using X-Ray Diffractogarm Method: Part 1. *Am. J. Nano Res. Appl.* **2020**, *8*, 58.
(37) Gale, M.; Nguyen, T.; Moreno, M.; Gilliard-AbdulAziz, K. L. Physiochemical Properties of Biochar and Activated Carbon from Biomass Residue: Influence of Process Conditions to Adsorbent Properties. *ACS Omega* **2021**, *6*, 10224−10233.
(38) Chen, T.; Liu, R.; Scott, N. R. Characterization of Energy Carriers Obtained from the Pyrolysis of White Ash, Switchgrass and Corn Stover - Biochar, Syngas and Bio-Oil. *Fuel Process. Technol.* **2016**, *142*, 124−134.

https://doi.org/10.1021/acsomega.2c04815
ACS Omega 2023, 8, 380−390